applied sciences

MDPI

Article

Phase Optimized Photoacoustic Sensing of Gas Mixtures

Mario Mordmueller [1], Simon Edelmann [2], Markus Knestel [2], Wolfgang Schade [1,3] and Ulrike Willer [1,*]

1 Institute for Energy Research and Physical Technology and Research Center Energy Storage Technologies, Clausthal University of Technology, Am Stollen 19B, 38640 Goslar, Germany; mario.mordmueller@tu-clausthal.de (M.M.); wolfgang.schade@hhi.fraunhofer.de (W.S.)
2 KNESTEL Technologie & Elektronik, Osterwalder Straße 12, 87496 Hopferbach, Germany; Simon.Edelmann@knestel.de (S.E.); Markus.Knestel@knestel.de (M.K.)
3 Fraunhofer Heinrich Hertz Institute, Am Stollen 19H, 38640 Goslar, Germany
* Correspondence: ulrike.willer@tu-clausthal.de; Tel.: +49-5321-3816-8421

Received: 1 December 2019; Accepted: 1 January 2020; Published: 7 January 2020

Abstract: In this paper, we report on the progress of the auto-triggered quartz-enhanced photoacoustic spectroscopy (QEPAS) technique which operates without external frequency generators and ensures permanent locking to the current resonance frequency of the tuning fork. This is obtained by incorporating the tuning fork in an oscillator circuit that autonomously oscillates at the present resonance frequency that shifts with changing environmental conditions, e.g., density and viscosity of the surrounding gas, temperature, and pressure. Both, the oscillation amplitude as well as the frequency can be read from the oscillator circuit. The photoacoustic signal appears as an offset of the electrically induced signal amplitude. Since the sum amplitude depends on the phase relation between the electrical and photoacoustic driving forces, the phase is permanently modulated, enabling the extraction of the photoacoustic component by use of a second lock-in amplifier stage which is being referenced with the phase modulation frequency. The functionality of this method is demonstrated for methane detection in a carbon dioxide atmosphere in a concentration range from 0 to 100% and ammonia in synthetic air employing a pulsed mid infrared QCL around 1280 cm^{-1}. The gas mixtures are motivated by the demands in biogas-analysis.

Keywords: photoacoustics; QEPAS; autotrigger

1. Introduction

Quartz-enhanced photoacoustic spectroscopy (QEPAS) is a type of photoacoustic spectroscopy which employs a piezoelectric quartz tuning fork instead of a microphone as a transducer. Since the introduction of the QEPAS-technique by Kosterev et al. in 2002 [1] it has emerged to be a very useful tool for photoacoustic detection of a manifold of gaseous substances. Further progress in QEPAS has been made in terms of using custom tuning forks with larger gaps and lower resonance frequencies to use light sources with larger focal diameters such as LEDs or THz-QCLs or by incorporating the photoacoustic cell and transducer, also called spectrophone, in a multipass cell to increase the power density and thus the sensitivity. A summary of achievements for different species and with respect to the used techniques can be found e.g., in the review articles by Patimisco et al. [2,3] and Ma [4]. For a simple QEPAS setup only a bare quartz tuning fork is required; however, in most spectrophones the tuning fork is additionally equipped with acoustic resonators [5]. Their use can improve the S/N-ratio of a QEPAS spectrophone by a factor of up to 30 [6]. For a QEPAS system using the first overtone mode, an enhancement factor of even 50 as compared to the bare tuning fork was reported [7].

On the other hand a strong coupling between the tuning fork and the acoustic resonator exists and the highest signals are achieved when the resonance frequencies of the tuning fork and the one of the acoustic resonator coincide. The resonance frequency of the acoustic resonator is essentially dependent on its length in relation to the velocity of sound. The most common approach is to use two cylindrical pipe elements sandwiching the tuning fork in a way that the radiation is aimed through both segments and between the prongs of the tuning fork. In this configuration best sensitivity is achieved when the length of a segment is between half and a quarter of the sound wavelength. However, since the tuning fork and the acoustic resonator react differently on changes in the environmental conditions the balanced condition is easily lost when the system is operated in real world scenarios.

Provided that the excitation laser addresses multiple species, the large dynamic range of photoacoustic spectroscopy enables the measurement of both, main components as well as trace gases of a gas mixture. This is one demand for biogas analysis. Therefore, we demonstrated that the system is able to measure methane in a carbon dioxide atmosphere (main components) as well as ammonia in small concentrations as present within the biogas.

Besides the compact size and the small measurement volume of only a few cubic centimeters the high Q-factor of the tuning fork is usually highlighted as an advantage of the QEPAS-technique in contrast to conventional photoacoustic spectroscopy which gives rise to the high sensitivity of a QEPAS-spectrophone. However, at the same time, the high Q-factor results in a sharp resonance curve and thus a careful setting of the laser's modulation frequency is required. Since the resonance frequency of the spectrophone is affected by environmental conditions such as pressure, temperature, and gas composition related density and viscosity, changes of these parameters can easily cause measurement errors. In this paper a new detection scheme for using both electrical and photoacoustic driving of the tuning fork and phase modulation of these two driving forces is discussed.

2. Materials and Methods

In a typical QEPAS setup a laser beam is focused between the prongs of the tuning fork (and if applicable through an acoustic resonator). The emission wavelength of the laser source is tuned to an absorption line of the target molecule and is additionally modulated with the resonance frequency or half the resonance frequency of the tuning fork depending on the modulation approach, 1f-amplitude modulation or 2f-wavelength modulation, respectively. This is usually done using a separate frequency generator with a precision of at least 0.1 Hz. The tuning fork is connected to a trans-impedance amplifier and the signal is then further amplified by a lock-in amplifier which is referenced by the frequency generator. To determine the correct modulation frequency, the frequency can be scanned in proximity of the expected resonance frequency while recording the signal amplitude of the spectrophone and thus obtaining a resonance curve with a maximum at the spectrophone's resonance frequency. The modulation frequency of the laser has to be realigned frequently if changes in environmental conditions such as pressure, temperature, and gas composition are expected. Even a complete recalibration might be necessary because of changes of the Q-factor if the environmental conditions change perceivably.

Many QEPAS systems provide the ability to record resonance curves non-photo-acoustically by directly exciting the tuning fork with the frequency generator as reported by Kosterev et al. [8]. This feature is typically used for presetting the modulation frequency before optical alignment of the spectrophone and for verifying the modulation frequency after changes in the environmental conditions, but not for the actual measurement. Figure 1 shows the signals for photoacoustic excitation (open red squares), for purely electrical excitation (solid green squares), and for simultaneous electrical and photo-acoustic excitation while the phase between them is altered (filled squares). For this feasibility study pure methane was excited by a cw quantum cascade laser operating at $\nu = 1276.85\ cm^{-1}$ using 2f-modulation. The amplitudes were set to 60 mV for electrical excitation and to 40 mV for photoacoustic excitation by adjusting the amplitude and the modulation width respectively. Figure 1 shows the resulting signal for simultaneous excitation when the phase of the laser modulation is varied from

$\varphi = -210°$ to $+210°$ while the phase of the electrical excitation is fixed. The sinusoidal sum signal varies between $R_{LI} = 20$ and 100 mV. The phase difference between two maxima is $\Delta\varphi = 180°$. Since the phase was set with respect to the modulation frequency which is half the resonance frequency of the tuning fork because of 2f-modulation the actual phase difference is 360°, as expected.

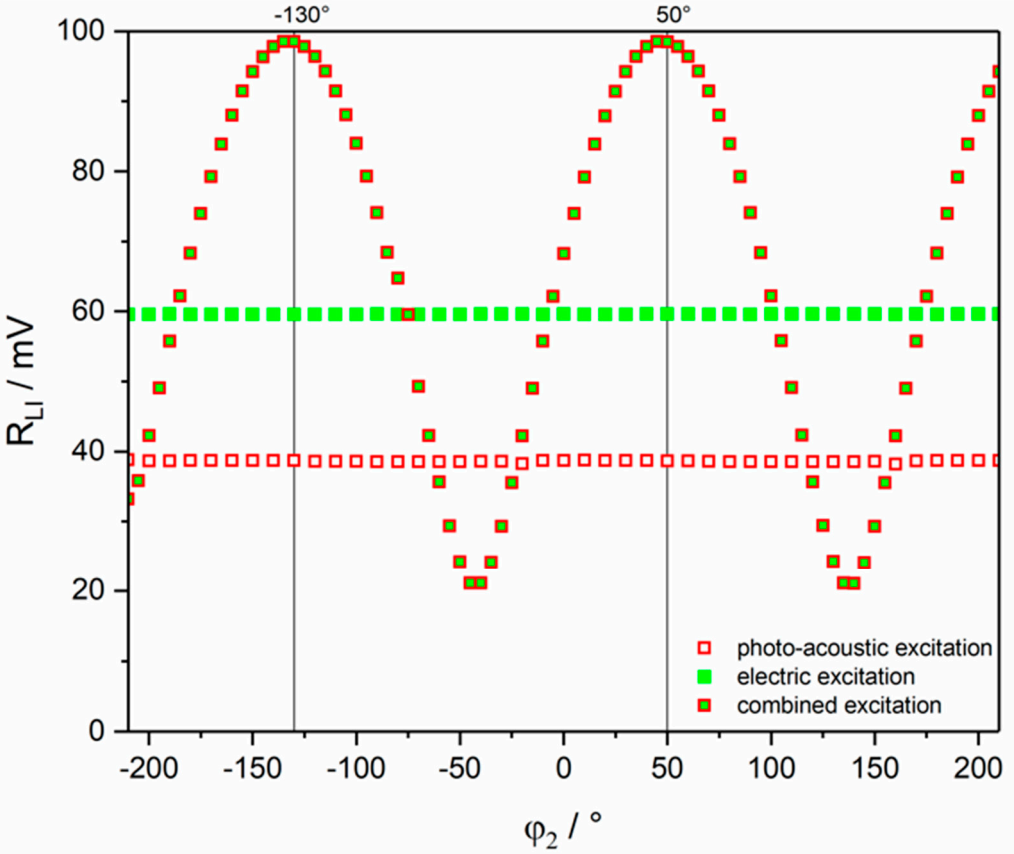

Figure 1. Generated signal amplitude at the lock-in-amplifier for photoacoustic excitation (open red squares), electrical excitation (solid green squares), and simultaneous excitation (green filled red squares). The latter depends on the phase between the two driving forces.

In [9,10] we already described the ability to incorporate a quartz micro-tuning fork with removed container in an oscillator circuit and to simultaneously focus a laser beam between the tuning fork's prongs to generate acoustic waves upon absorption of the molecule. Since the laser modulation signal is derived from the oscillation circuit that automatically adjusts to the current resonance frequency of the tuning fork, the laser is always modulated with the correct frequency. The measurement signal and the reference which are fed to the lock-in amplifier are also derived from the oscillator circuit. The measurement signal is thus the sum of the electrically generated amplitude and the photo-acoustically induced amplitude, which furthermore depends on the phase between both signals. Until now, the phase was manually adjusted as a temporal delay in the modulation line to obtain a maximum signal amplitude. A scheme of this method is shown in Figure 2a. The phase of a photoacoustic wave is governed by the gas mixture's relaxation dynamics which in turn depends on the collision partner behavior and thus on the gas mixture composition, its pressure and temperature. Therefore a phase setting optimized for a fixed concentration is valid for a limited range of the mentioned parameters only. This partially limits the advantage of the modulation frequency auto tracking: instead of the realignment of the frequency a realignment of the phase is needed. In this paper however, we report on the ability of a continuous phase modulation instead of a fixed setting which yields a steady measurement and additionally separates the photo-acoustically induced amplitude from the offset generated by the oscillator circuit.

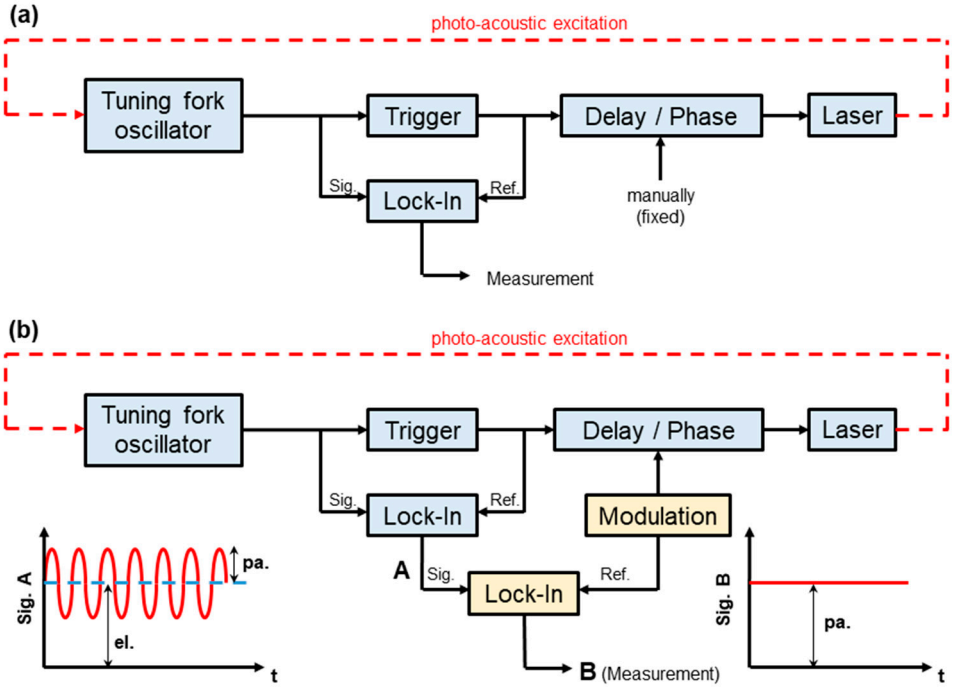

Figure 2. Schematic of the setup for modulation frequency auto tracking: (**a**) the tuning fork oscillator adjusts to the present resonance frequency. This is fed as reference to the lock-in amplifier and with a manually set (fixed) phase to the laser driver for modulation. The signal output at the lock-in is the sum of photoacoustic and electrical excitation. (**b**) A second lock-in amplifier is added to the setup and the phase of the laser modulation is modulated with a lower frequency. Thus the signal A of the first lock-in shows a sinusoidal variation (left inset). The second lock-in demodulates and amplifies this signal and yields a constant signal B (right inset) which is proportional to the sole photoacoustic excitation.

Figure 2b depicts how the auto-triggered QEPAS setup can be extended to avoid the critical phase alignment. Instead of setting a fixed delay the phase is continuously modulated between 0 and 360° with a frequency f_{phs} = 0.37 Hz which is considerably smaller than the resonance frequency of the tuning fork. The output (A) of the first lock-in amplifier is fed to the input of a second lock-in amplifier which is referenced with the phase modulation frequency f_{phs}. Without target molecules present in the spectrophone, signal (A) represents the amplitude induced by the oscillator circuit only. It is not modulated and thus output (B) of the second lock-in-amplifier is zero. Upon absorption, signal (A) starts oscillating with the frequency f_{phs} and the photo-acoustically induced amplitude. The output of the second lock-in amplifier (B) shows the oscillation amplitude of (A), i.e., the pure photo-acoustic amplitude without electrically induced offset.

The functionality of the two lock-in stages was incorporated into one device developed by KNESTEL Technologie & Elektronik GmbH. The device consists of a combination of a micro controller and a FPGA where the functionality of both lock-in amplifiers and phase modulation is digitally programmed.

For the measurements detailed in Section 3, a pulsed external cavity QCL provided by the Fraunhofer IAF was used because it covers both, methane and ammonia which are important for biogas measurements. The laser emits pulses at a repetition rate f_{rep} = 400 kHz and is over-modulated with a TTL signal with a duty cycle of roughly 30% (either generated by the oscillator circuit or manually set) thus releasing four laser pulses during each high-level. The laser can be tuned in the frequency range 980 cm^{-1}–1290 cm^{-1}.

A spectrophone without acoustic resonators was used for the measurements, which were conducted at ambient pressure and room temperature.

3. Results

3.1. Influence of Background Gas Mixture

Figure 3a compares the results of measurements of methane in carbon dioxide in a concentration range between C_{CH4} = 0% and 100% using the three different methods: (1) the aforementioned device, (2) the autotrigger-approach without phase modulation, and (3) data extracted from the resonance curves employing conventional QEPAS; the resonance curves are given in Figure 3b. Methane was excited at ν = 1276.85 cm^{-1}.

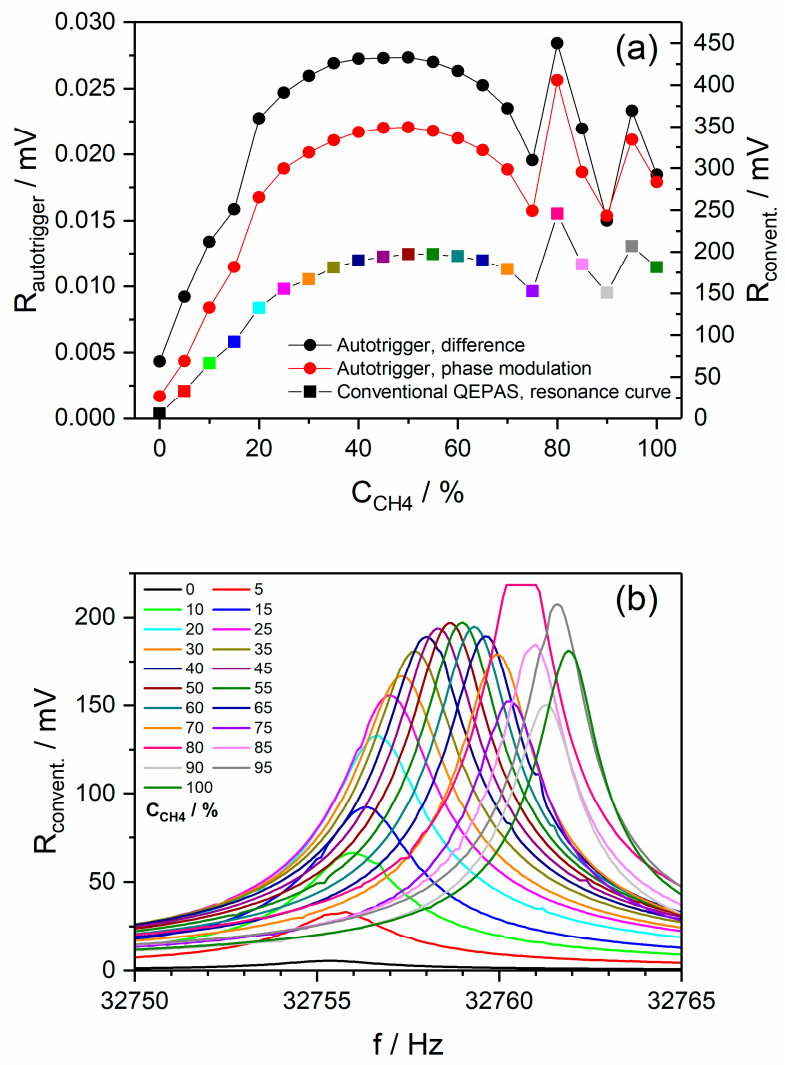

Figure 3. (**a**) Comparison of results achieved with three different measurement techniques: black dots: autotrigger measurement with fixed phase. The values are derived by subtraction of measurements with blocked laser from those with photoacoustic excitation. Red dots: reading of lock-in amplifier 2 using phase modulation. Colored dots: values extracted from conventional quartz-enhanced photoacoustic spectroscopy (QEPAS) resonance curves given in (**b**) in the respective color. (**b**) Resonance curves for different mixtures of methane and carbon dioxide.

The black dots show the differences of measurements with and without photoacoustic excitation with manually set phase difference as depicted in the schematic in Figure 2a. The phase difference was adjusted at a concentration of C_{CH4} = 50% to maximize the signal. The difference represents the photo-acoustically induced component of the signal. The red dots show a measurement performed with the phase modulation approach sketched in Figure 2b and the composition of colored symbols

is extracted from the measurement of whole resonance curves which are given in Figure 3b in the respective colors. The three measurement methods show similar results disregarding a slight offset which is probably due to the different electric circuits used. The photoacoustic signal is proportional to the laser power absorbed in the vicinity of the tuning fork. Since the concentrations are high, the lambert–beer law which governs the absorption cannot be linearized as for trace gases and a nonlinear increase of the signal is expected. The Q-factor changes as the mixture of methane and carbon dioxide is altered. An increase in Q-factor is observed for increasing methane concentrations. On the other hand, not all the output power of the laser reaches the tuning fork; the higher the concentrations get, the more laser radiation is absorbed on the optical path before the tuning fork which is roughly 4 mm long. This leads to a decrease in signal since only the acoustic waves generated between the prongs excite the piezoelectric active oscillation. This explains the maximum of the curve and its decrease at higher concentrations. The part of the curve for concentrations higher than 70% shows two peaks that cannot be explained with the nonlinear absorption behavior but is consistent with all three measurement methods. They are either due to changes in relaxation dynamics or acoustic resonances inside the spectrophone body and will be further analyzed.

3.2. Sensing Limit

The method was originally developed to meet the difficulties of changing environmental conditions caused by considerable concentration changes of either the analyte itself or the gas matrix around. For the application in biogas detection, it is also needed to measure trace components as ammonia with the same device. This section therefore investigates its application for the measurement of small concentrations and for this purpose ammonia was measured in the range between 1060 cm^{-1} and 1150 cm^{-1} employing the same laser source. Figure 4 shows in green the simulated absorption coefficient derived from HITRAN [11] for 1.5% ammonia in synthetic air. The signal of the second lock-in amplifier is shown in red, i.e., the pure photoacoustic signal is given and the measurement of the power transmitted through the cell is depicted in black for comparison.

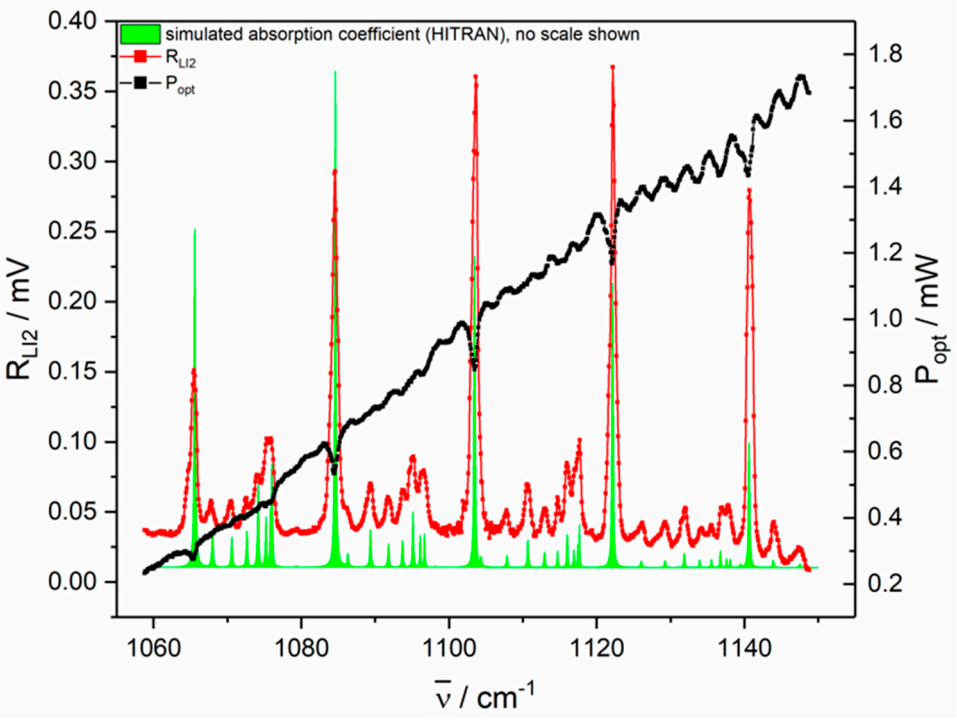

Figure 4. Comparison of transmitted power (black), photoacoustic signal (red), and simulated absorption (green) for 1.5% ammonia in synthetic air.

The gas mixture was further diluted and the signal of the peak at 1103.6 cm^{-1} was further analyzed. Each point in Figure 5 is the mean value of 101 single measurements and the error bars represent the standard deviation for each concentration. The mean value of the standard deviation is 1.62 µV. A linear dependence of the signal on the concentration is found for concentrations up to 1.1%. The limit of detection was derived to be 246 ppm using a 3σ margin. This is sufficient for the application since ammonia is present in the biogas in concentrations up to 1%. Dang et al. describe a system optimized for the detection of ammonia with a custom tuning fork and they achieve a sensing limit of 22 ppm [12]. Ma et al. reached 418 ppb using a custom tuning fork and an amplified source [13] and Wu et al. even reached 17 ppb, also with an amplified excitation source [14].

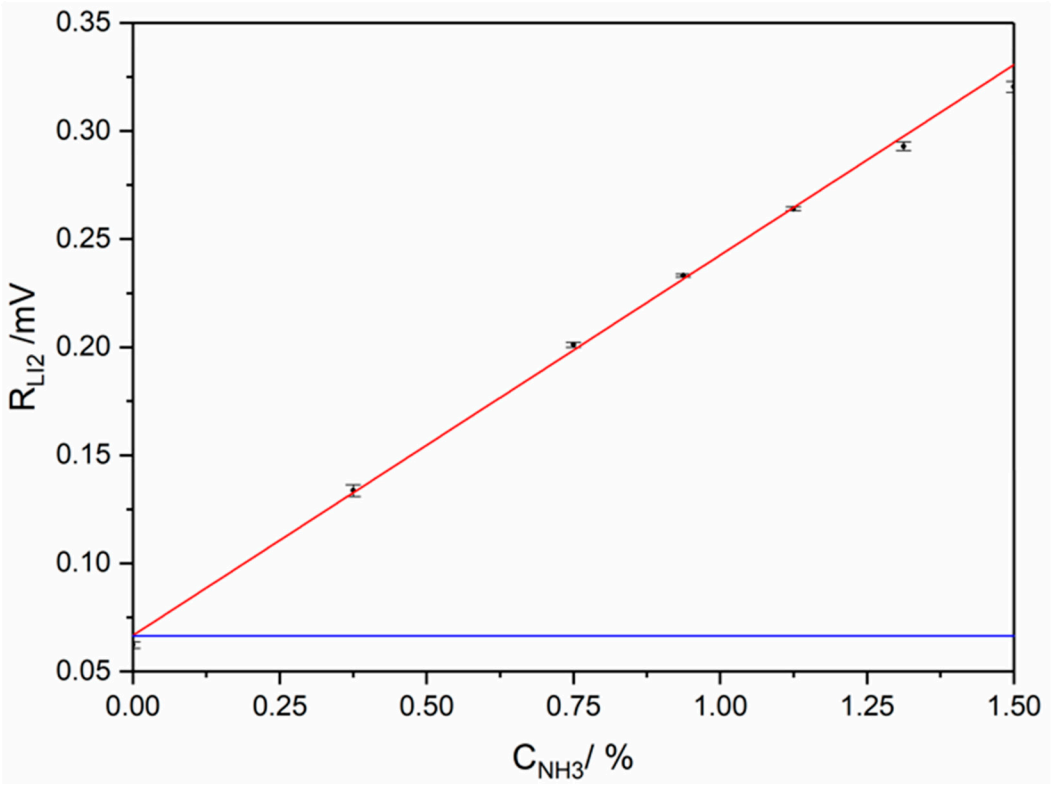

Figure 5. Determination of the limit of detection of NH_3 in synthetic air. The blue line marks the sum of the mean value of the noise floor and 3 times its standard deviation.

4. Discussion

A considerable optimization for the dual excitation technique for QEPAS has been introduced that ensures an automated adaption of the modulation frequency of the excitation laser to the resonance frequency of the tuning fork as well as signal retrieval at the optimum phase between electrical and photoacoustic excitation. Thus the pure photoacoustic signal is measured even though a simultaneous electrical driving is present. The performance was demonstrated using high methane concentrations varying from 0% to 100% in carbon dioxide. As for conventional QEPAS a linear dependence of the signal on the concentration is found for small concentration, which was demonstrated by the measurement of ammonia in synthetic air. The derived limit of detection is worse than for conventional QEPAS with acoustic resonator; however, the technique enables continuous measurement because no interruptions to check or realign the modulation frequency are needed.

Author Contributions: Conceptualization, M.M. and U.W.; data curation, M.M.; formal analysis, M.M. and U.W.; funding acquisition, M.K. and U.W.; investigation, M.M.; methodology, M.M. and U.W.; project administration, M.K. and U.W.; software, S.E. and M.K.; supervision, M.K., W.S., and U.W.; validation, M.M., S.E., and U.W.; visualization, M.M.; writing—original draft, M.M. and U.W.; writing—review and editing, S.E., M.K., and W.S. All authors have read and agreed to the published version of the manuscript.

Funding: This research was funded by Bundesministerium für Bildung und Forschung (German Federal Ministry of Education and Research), grant numbers 13N13826 and 13N13824.

Acknowledgments: We acknowledge support by Open Access Publishing Fund of Clausthal University of Technology.

Conflicts of Interest: The authors declare no conflict of interest.

References

1. Kosterev, A.A.; Bakhirkin, Y.A.; Curl, R.F.; Tittel, F.K. Quartz-enhanced photoacoustic spectroscopy. *Opt. Lett.* **2002**, *27*, 1902–1904. [CrossRef] [PubMed]
2. Patimisco, P.; Scamarcio, G.; Tittel, F.K.; Spagnolo, V. Quartz-enhanced photoacoustic spectroscopy: A review. *Sensors* **2014**, *14*, 6165–6206. [CrossRef] [PubMed]
3. Patimisco, P.; Sampaolo, A.; Dong, L.; Tittel, F.K.; Spagnolo, V. Recent advances in quartz enhanced photoacoustic sensing. *Appl. Phys. Rev.* **2018**, *5*, 11106. [CrossRef]
4. Ma, Y. Review of Recent Advances in QEPAS-Based Trace Gas Sensing. *Appl. Sci.* **2018**, *8*, 1822. [CrossRef]
5. Zheng, H.; Dong, L.; Wu, H.; Yin, X.; Xiao, L.; Jia, S.; Curl, R.F.; Tittel, F.K. Application of acoustic micro-resonators in quartz-enhanced photoacoustic spectroscopy for trace gas analysis. *Chem. Phys. Lett.* **2018**, *691*, 462–472. [CrossRef]
6. Dong, L.; Kosterev, A.A.; Thomazy, D.; Tittel, F.K. QEPAS spectrophones: Design, optimization, and performance. *Appl. Phys. B* **2010**, *100*, 627–635. [CrossRef]
7. Zheng, H.; Dong, L.; Sampaolo, A.; Patimisco, P.; Ma, W.; Zhang, L.; Yin, W.; Xiao, L.; Spagnolo, V.; Jia, S.; et al. Overtone resonance enhanced single-tube on-beam quartz enhanced photoacoustic spectrophone. *Appl. Phys. Lett.* **2016**, *109*, 111103. [CrossRef]
8. Kosterev, A.A.; Bakhirkin, Y.A.; Tittel, F.K. Ultrasensitive gas detection by quartz-enhanced photoacoustic spectroscopy in the fundamental molecular absorption bands region. *Appl. Phys. B* **2005**, *80*, 133–138. [CrossRef]
9. Mordmüller, M.; Köhring, M.; Schade, W.; Willer, U. An electrically and optically cooperated QEPAS device for highly integrated gas sensors. *Appl. Phys. B* **2015**, *119*, 111–118. [CrossRef]
10. Mordmueller, M.; Schade, W.; Willer, U. QEPAS with electrical co-excitation for photoacoustic measurements in fluctuating background gases. *Appl. Phys. B* **2017**, *123*, 1902. [CrossRef]
11. Rothman, L.S.; Rinsland, C.P.; Goldman, A.; Massie, S.T.; Edwards, D.P.; Flaud, J.-M.; Perrin, A.; Camy-Peyret, C.; Dana, V.; Mandin, J.-Y.; et al. The Hitran Molecular Spectroscopic database and Hawks (Hitran Atmospheric Workstation): 1996 Edition. *J. Quant. Spectrosc. Radiat. Transf.* **1998**, *60*, 665–710. [CrossRef]
12. Dang, H.; Ma, Y.; Liu, F.; Lu, J. Sensitive Detection of Ammonia Based on Quartz-Enhanced Photoacoustic Spectroscopy. *J. Russ. Laser Res.* **2019**, *40*, 265–268. [CrossRef]
13. Ma, Y.; He, Y.; Tong, Y.; Yu, X.; Tittel, F.K. Ppb-level detection of ammonia based on QEPAS using a power amplified laser and a low resonance frequency quartz tuning fork. *Opt. Express* **2017**, *25*, 29356. [CrossRef]
14. Wu, H.; Dong, L.; Liu, X.; Zheng, H.; Yin, X.; Ma, W.; Zhang, L.; Yin, W.; Jia, S. Fiber-amplifier-enhanced QEPAS sensor for simultaneous trace gas detection of NH_3 and H_2S. *Sensors* **2015**, *15*, 26743–26755. [CrossRef] [PubMed]